Charge Transfer Analysis of 2p3d Resonant Inelastic X-ray Scattering of Cobalt Sulfide and Halides

Ru-Pan Wang,[†] Boyang Liu,[†] Robert Green,[‡] Mario Ulises Delgado-Jaime,[†] Mahnaz Ghiasi,[†] Thorsten Schmitt,[§] Matti M. van Schooneveld,[†,*1] and Frank M. F. de Groot[†,*2]

[†]Inorganic Chemistry & Catalysis, Debye Institute for Nanomaterials Science, Utrecht University, Universiteitsweg 99, 3584 CG, Utrecht, The Netherlands

[‡]Department of Physics & Astronomy, University of British Columbia, V6T 1Z1 Vancouver, Canada

[§]Paul Scherrer Institut, Swiss Light Source, CH-5232 Villigen PSI, Switzerland

1. Applied X-ray Skin Doses

Table S1. Total Acquisition Times for Each RIXS Spectrum.

	Total exposure time (s)					
Excitation energy	**A**	**B**	**C**	**D**	**E**	**F**
CoF_2	600	600	600	600	600	600
$CoCl_2$	900	400	400	350	900	900
$CoBr_2$	360	450	450	450	900	900
CoS	1200	-	900	900	1200	1200

[*1] Corresponding author: M.M.vanschooneveld@gmail.com

Tel: (+31) 302537400

[*2] Corresponding author: F.M.F.deGroot@uu.nl

Tel: (+31) 302537400

2. Charge Transfer Multiplet Calculation and Single Impurity Anderson Model

In a Charge Transfer Multiplet (CTM) calculation, the system is built up from an ionic model with an external ligand potential. The Hamiltonian of the system can be described as:

$$H = H_{ionic} + V_{CF} = \sum T_e + V_{p-e} + \sum V_{e-e} + V_{SOC} + V_{CF}, \quad \text{(s1)}$$

where T_e is the kinetic energy of the electrons, V_{p-e} is the attractive potential energy between electrons and the nucleus, and V_{e-e} is the interaction potential energy from surrounding electrons. The solutions are given in terms of the atomic orbital basis, where double group symmetries are used to take the spin-orbit coupling into account (V_{SOC}). This basis set is obtained with a Slater determinant as calculated with a scaled Hartree-Fock approximation. The degenerated states will be split according to the V_{CF} term. For example, the octahedral crystal field potential will split the 3d states into the e_g and t_{2g} states.

The LMCT effect was calculated by the Single Impurity Anderson Model (SIAM) with interaction between configurations d^n and $d^{n+1}\underline{L}$, where an electron has been transferred from the ligand valence band while preserving spin and symmetry. The charge transfer energy (Δ) is the ionic energy difference between the two configurations and the electron hopping integrals (T) describe their coupling. An interacting operator H_{mix} is applied in SIAM, yielding the Hamiltonian matrix:

$$H' = H + H_{mix} = \begin{bmatrix} \mathrm{E}_{d_j^n} & \mathrm{T}_j \\ \mathrm{T}_j & \mathrm{E}_{d_j^{n+1}\underline{L}} + \Delta \end{bmatrix}, \text{ where } H_{mix} = \begin{bmatrix} 0 & \mathrm{T}_j \\ \mathrm{T}_j & \Delta \end{bmatrix}. \quad \text{(s2)}$$

The symbol *j* presents the irreducible symmetry group of the state. For example, the state with E_g orbital symmetry presents e_g states. The energy difference between two configurations within the same symmetry group is defined as $\mathrm{dE}_j = \mathrm{E}_{d_j^{n+1}\underline{L}} - \mathrm{E}_{d_j^n}$. The eigenenergies ($\mathrm{E}_{\pm,j}$) and wave functions ($|\varphi_\pm>$) of this new Hamiltonian are:

$$\mathrm{E}_{\pm,j} = \frac{1}{2}\left(2\mathrm{E}_{d_j^n} + \mathrm{dE}_j + \Delta \pm \sqrt{\left(\mathrm{dE}_j + \Delta\right)^2 + 4\mathrm{T}_j^{\,2}}\right)$$

$$\text{and } \left|\varphi_{\pm,j}\right> = \alpha_{\pm,j}\left|d_j^n\right> + \beta_{\pm,j}\left|d_j^{n+1}\underline{L}\right>. \quad \text{(s3)}$$

The solution with a negative (positive) sign has a lower energy and corresponds to the bonding (anti-bonding) state. The wave functions were simplified as $|\varphi_{GS}> = \alpha|d^n> + \beta|d^{n+1}\underline{L}>$ with a eigenenergy E_{GS}. The value $(\mathrm{dE}_i + \Delta)$ is an effective charge transfer energy Δ_{eff}. The energy difference between bonding and anti-bonding states of the same orbital symmetry is almost linear dependent on Δ_{eff}. The hybridization percentages of the two

states are obtained from $|\alpha_{\pm}|^2$ and $|\beta_{\pm}|^2$. However, more generally, the multi-electron configuration should be concerned. The actual states will be linear combinations of few configurations with different orbital symmetries. In an octahedral symmetry, the strong field configuration projections can be described in terms of e_g and t_{2g} states. For a Co^{2+} ion in an octahedral field, the bonding state of configuration yields:

$$|\varphi_- >= \sum \alpha_{-,s}|e_g^{7-s}t_{2g}^{s}> + \sum \beta_{-,t}|e_g^{8-t}t_{2g}^{t}\underline{L}>, \quad \text{(s4)}$$

$$P(d_i^7) = |\alpha_-|^2 = \sum_{6\geq s\geq 3}|\alpha_{-,s}|^2 = P\left(e_g^{7-s}t_{2g}^{s}\right), \quad \text{(s5)}$$

$$\text{and } P(d_i^8\underline{L}) = |\beta_-|^2 = \sum_{6\geq t\geq 4}|\beta_{-,t}|^2 = P\left(e_g^{8-t}t_{2g}^{t}\underline{L}\right). \quad \text{(s6)}$$

Where the indices *s* and *t* are the number of electrons in the t_{2g} states and P gives the corresponding population of the states. As mentioned above, the actual states will be linear combinations of $e_g^{7-s}\,t_{2g}^{s}$ configurations due to multiplet effects and spin-orbit coupling. From this, the covalency of the e_g and t_{2g} states can be calculated from these electron distributions. Following equation (s3), the difference between two states with different symmetry group *k* and *l* is given by:

$$\Delta E\left(10Dq_{eff}\right) \equiv \Delta E_{l-to-k}$$

$$= \frac{1}{2}\left\{2E_{d_k^n} - 2E_{d_l^n} + dE_k - dE_l - \left(\sqrt{(dE_k+\Delta)^2 + 4T_k{}^2} - \sqrt{(dE_l+\Delta)^2 + 4T_l{}^2}\right)\right\}. \quad \text{(s7)}$$

In a single electron model, *k* and *l* are replaced by e_g and t_{2g} states, respectively. The energy difference between e_g and t_{2g} states is defined as a crystal field splitting energy ($10Dq_{eff}$). The term $2E_{d_k^n} - 2E_{d_l^n} + dE_k - dE_l$ is defined as $\Delta E(10Dq_{ion})$, which is the energy difference of the ionic states and is determined only by a given ionic crystal field splitting energy ($10Dq_{ion}$). Subtracting it from $\Delta E\left(10Dq_{eff}\right)$ and replacing *k* as e_g and *l* as t_{2g}, yields a part that remain dependent on Δ. Thus, this energy difference can be rewritten as:

$$\Delta E_{CT} = \frac{1}{2}\left\{\sqrt{\left(dE_{t_{2g}}+\Delta\right)^2 + 4T_{t_{2g}}{}^2} - \sqrt{\left(dE_{e_g}+\Delta\right)^2 + 4T_{e_g}{}^2}\right\}. \quad \text{(s8)}$$

Equation (s8) shows an extra energy difference between e_g and t_{2g} states and implies that the crystal field of our system is affected. In a weak charge transfer system ($i.e., \Delta \gg |T_{t_{2g}}| \cong |T_{e_g}|$), the value of ΔE_{CT} is negligible. Under these conditions, this system can be treated as ionic case. More general, all the $e_g^{7-s}\,t_{2g}^{s}$ configurations should be considered in a multi-

electron model. Equation (s8) would be extended with more Δ-depending terms. Nevertheless, a linear function can approximate this relation when the energy difference is small.

As a result, the effective splitting energy ($10\mathrm{Dq}_{eff}$) between the t_{2g} and the e_g states is dependent on the charge transfer energy Δ. From this, it follows that expression s7 can be rewritten with the following equation (equation (2) in the main article):

$$\Delta\mathrm{E}\left(10\mathrm{Dq}_{eff}\right) = \Delta\mathrm{E}(10\mathrm{Dq}_{ion}) + \Delta\mathrm{E}_{CT}(\Delta). \quad \text{(s9)}$$

3. Details on the Experimental and Simulated Results

In this section, more spectral details are presented.

a. Term-symbol Identities

Based on the calculations, the Mulliken symbols are indicated. In the bottom panels of Figure S1, state term-symbols are given in comparison with the RIXS spectra at energy F. The state energies are given in Table S2. The comparisons between the experiments and simulations are shown in the top panels.

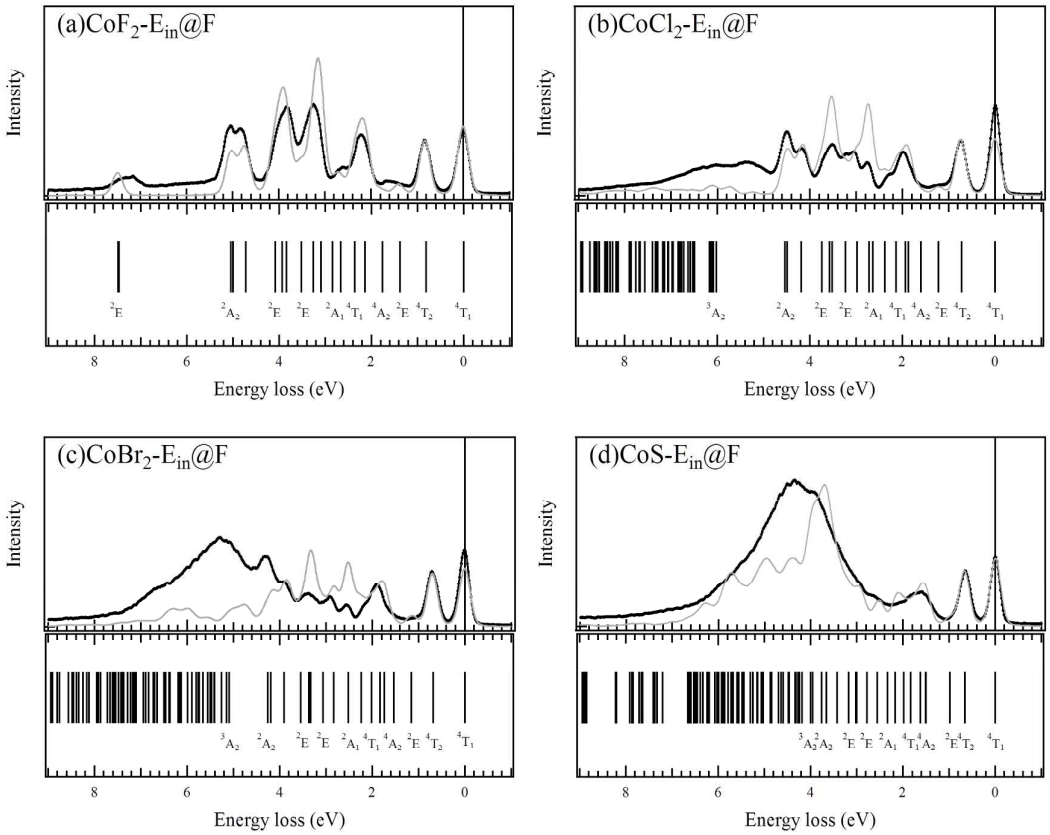

Figure S1. Calculated energy diagrams of (a) CoF_2, (b) $CoCl_2$, (c) $CoBr_2$, and (d) CoS compared to corresponding 2p3d RIXS calculated (gray solid lines) and experimental results (black solid lines).

b. Incident Energy Dependent Behaviors

All the spectra at the selected incident energies are presented, in which the spectra with the incident energies A, D, F, and G are discussed in the main text. The spectral features were resonating differently with varying incident photon energies according to the Kramers-Heisenberg formula. At energies A to E, the dd-excitations of spin quartet states ($^4T_1$, $^4T_2$, $^4A_2$) dominated the spectra. The charge transfer excitations are the features has been indicated as $^3A_2$ states or the states with an energy higher than it. Other possible observed states between 1.5 and 4 eV are the spin doublet states (Table S2). For example, because of the incident energy selectivity, a feature about 1.3 eV (^2E states) is appeared at energy F in CoF_2.Whereas, at the energy A, mainly the 1.7 eV feature ($^4A_2$ states) contributes the intensity (Figure S2a). Similar behavior can be also observed for $CoCl_2$ and $CoBr_2$(Figure S2b and S2c)). By comparing the features between the spectra at different incident energies, more orbital information can be obtained.

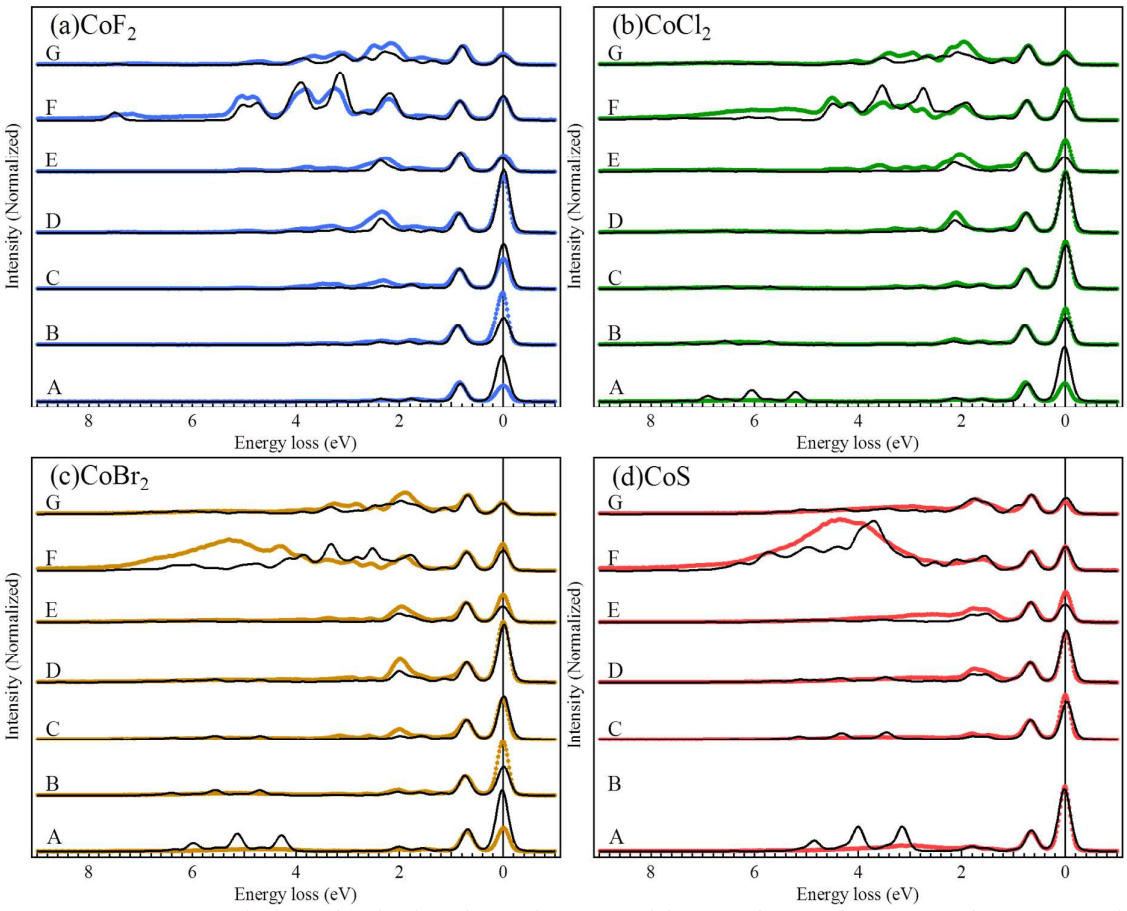

Figure S2. Comparisons of calculated 2p3d RIXS with experimental spectra of (a) CoF_2, (b) $CoCl_2$, (c) $CoBr_2$, and (d) CoS. The black lines are the simulation with the charge transfer effect on.

The charge transfer excitations are a "band-like" features and consequently broadened by a width W. In simulation, the best simulated W was 2.2 eV obtained from the center of mass of the antibonding states. Due to limitations in calculating power, only 3 splitting states were considered to calculate W instead of a band (infinite states should be considered). For example, 3 separated peaks about 3, 4, 5 eV appear in the calculation results for CoS (Figure S2d). These 3 states still represent the LMCT effect on the lowest, the central, and the highest edge of the band.

Table S2. The RIXS State Symmetry Term Labels and Energies (in eV) Derived from Experiment and Calculation Results

	CoF2	**CoCl2**	**CoBr2**	**CoS**
	Exp / Cal	**Exp / Cal**	**Exp / Cal**	**Exp / Cal**
Quartet				
$^4T_1$	0.00 / 0.00	0.00 / 0.00	0.00 / 0.00	0.00 / 0.00
$^4T_2$	0.85 / 0.81	0.77 / 0.72	0.71 / 0.68	0.67 / 0.65
$^4A_2$	1.71 / 1.76	1.60 / 1.61	1.52 / 1.54	1.44 / 1.51
$^4T_1$	2.27 / 2.35	2.11 / 2.14	1.98 / 2.02	1.79 / 1.83
Doublet				
^2E	1.33 / 1.37	1.21 / 1.22	1.11 / 1.15	- / 0.98
$^2T_1$	- / 2.13	- / 1.93	- / 1.83	- / 1.62
$^2T_2$	- / 2.13	- / 1.87	- / 1.74	- / 1.49
$^2T_1$	2.63 / 2.67	2.25 / 2.38	2.15 / 2.20	- / 1.98
$^2A_1$	- / 2.84	- / 2.63	- / 2.51	- / 2.33
$^2T_2$	- / 3.09	2.76 / 2.72	2.59 / 2.52	2.13 / 2.16
$^2T_1$	3.25 / 3.26	3.10 / 2.98	2.94 / 2.83	2.59 / 2.56
^2E	3.50 / 3.51	3.24 / 3.23	3.15 / 3.06	- / 2.77
$^2T_2$	- / 3.84	- / 3.51	- / 3.33	- / 3.01
$^2T_1$	3.84 / 3.94	3.57 / 3.57	3.38 / 3.36	2.98 / 3.00
^2E	- / 4.08	- / 3.74	- / 3.54	3.19 / 3.18
$^2T_2$	4.88 / 4.72	4.12 / 4.18	3.95 / 3.91	- / 3.43
$^2T_1$	- / 4.99	4.49 / 4.46	- / 4.19	- / 3.65
$^2A_2$	5.15 / 5.04	4.63 / 4.54	4.30 / 4.25	- / 3.76
$^2E/^2T_2/^2T_1$	7.30 / 7.47	5.40 / -		
Charge Transfer				
$^3A_2$ **(CT)**	11.50 / 11.26	6.12 / 6.11	5.30 / 5.30	3.94/ 4.20

c. Comparing the Calculation with and without Charge Transfer Effect

The calculations without charge transfer effect were generated by reducing the Slater integrals. The initial setting of atomic initial Slater integral values were given as: F^2_{dd} = 9.284 eV and F^4_{dd} = 6.678 eV for $2p^63d^7$ configuration and F^2_{dd} = 9.917, F^4_{dd} = 7.140, F^2_{pd} = 5.808, G^1_{pd} = 3.886, and G^3_{pd} = 2.455 eV. These values have been reduced by 80% from the Hartree-Fock approximation. The F_{dd} reduction percentages were used as 95%, 85.5%, 83.1%, and 71.3% for CoF_2, $CoCl_2$, $CoBr_2$, and CoS, respectively. The main features of 2p XAS were reproduced well in both simulations (Figure S3). However, the LMCT satellite peaks, which are indicated as CT in the figures, are not found in the ionic simulation. These peaks were not clearly visible due to the considerable ligands' p band broadening of $2p^53d^8\underline{L}$ configuration, where 2.2 eV was used in the calculations. Note that in the LMCT simulation the Slater integrals values F^2_{dd}, F^4_{dd}, F^2_{pd}, G^1_{pd}, and G^3_{pd} are 82%, 94%, 88%, 80%, and 88% of the Hartree-Fock values, respectively.

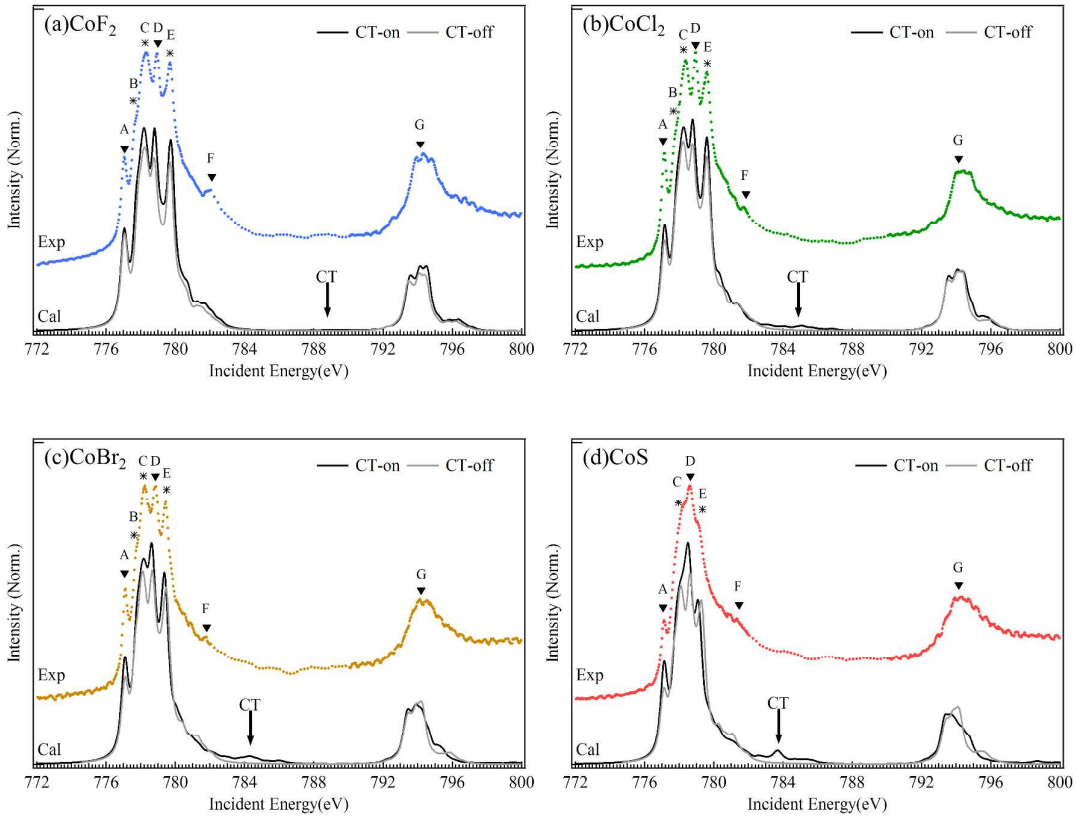

Figure S3. Comparisons of calculated 2p3d XAS spectra with experimental spectra of (a) CoF_2, (b) $CoCl_2$, (c) $CoBr_2$, and (d) CoS. The black and gray lines are the simulation with and without the charge transfer effect, respectively.

The calculations without charge transfer effect give no anti-bonding features (Figure S4) although the bonding features can reproduced well.

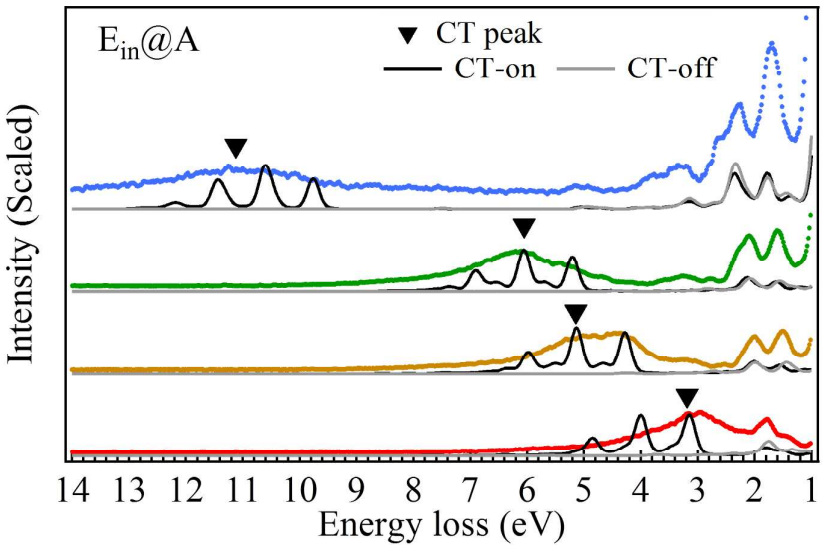

Figure S4. Comparisons of calculated 2p3d XAS spectra with and without charge transfer effect to the experimental spectra.

4. Tanabe-Sugano Diagrams and the Effects of Charge Transfer

a. Tanabe-Sugano Diagram Without Charge Transfer Effect

For a $3d^7$ ion, the O_h crystal field split the orbital into e_g and t_{2g} states. Considering the multi-election interactions, the energy levels of $3d^7$ can be described as a function of crystal field energy (10Dq). Figure S5 gives the energy diagram, so-called Tanabe-Sugano diagram, of the $3d^7$ configuration. In this diagram, the states are split by the crystal field value 10Dq without considering charge transfer effects. The energies of the excitation states vary almost linearly with 10Dq between 0.2 - 1.3 eV. Note that the Slater integrals values F^2_{dd}, F^4_{dd}, F^2_{pd}, G^1_{pd}, and G^3_{pd} are 82%, 94%, 88%, 80%, and 88% of the Hartree-Fock values, respectively.

Figure S6 shows the 2p3d RIXS simulated spectra (without charge transfer effects). We use the $^4T_2$ state to trace our experimental result. The $^4T_2$ excitation energies as function of $10Dq_{ion}$ are shown in Table S3. The $^4T_2$ peak positions are a bit higher than the lowest $^4T_2$ state in Figure S5. This is because of the spin-orbit coupling has be included in Figure S6. In a model without charge transfer, $10Dq_{ion}$ is the same as $10Dq_{eff}$. In other words, the first dd-excitation ($^4T_1$ to $^4T_2$ excitation) can be directly related to $10Dq_{eff}$. However, more generally, the multi-electron configuration should be concerned.

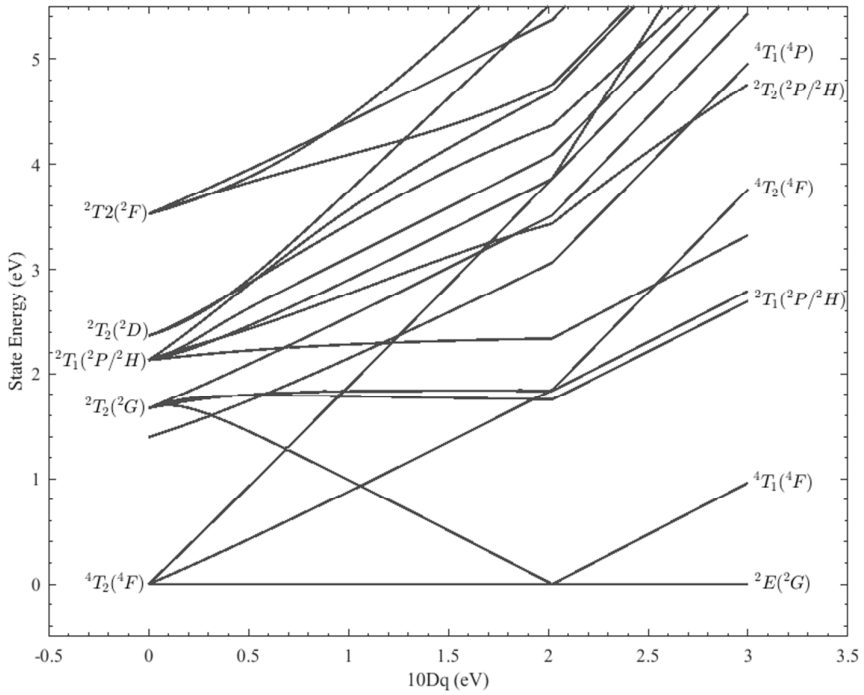

Figure S5. Tanabe-Sugano diagram of the d^7 configuration.

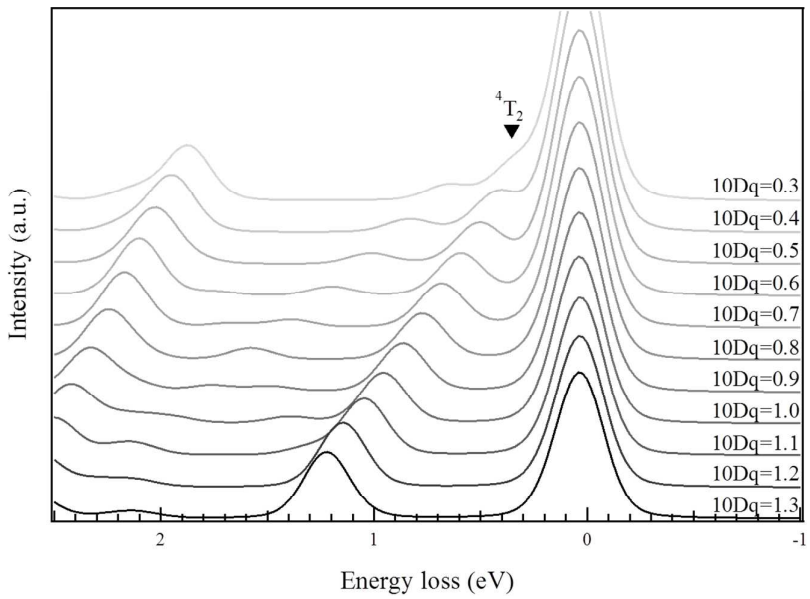

Figure S6. 2p3d RIXS simulated spectra at a constant excitation energy with $10Dq_{ion}$ floating from 0.3 to 1.3 eV without charge transfer effect.

Table S3. The First dd-excitation Energy w.r.t $10Dq_{ion}$(=$10Dq_{eff}$)

$10Dq_{ion}$	$^4T_1$	$10Dq_{ion}$	$^4T_1$	$10Dq_{ion}$	$^4T_1$
0.3	0.32	**0.7**	0.65	**1.1**	1.01
0.4	0.39	**0.8**	0.75	**1.2**	1.13
0.5	0.47	**0.9**	0.83	**1.3**	1.18
0.6	0.57	**1.0**	0.93		

b. Excitation Energies with Charge Transfer Effects in the SIAM

In order to understand the extra crystal field energy shift due to charge transfer hybridization, RIXS spectra with different crystal field values ($10Dq_{ion}$) and charge transfer energies (Δ) are calculated. This extra crystal field energy shift is referred to as ΔE_{CT}. Figure S7 shows the results which correspond to a $10Dq_{ion}$ value of 0.75 eV. We selected the $^4T_2$ state and used equation (s10) in next subsection to convert the excitation energy back to $10Dq_{eff}$. Then the ΔE_{CT} values could be worked out by subtracting the $10Dq_{ion}$ from $10Dq_{eff}$. This process was repeated by changing the $10Dq_{ion}$ value equal to 0.75 eV and 1.0 eV, from which the corresponding ΔE_{CT} values are obtained. All these ΔE_{CT} values are given in Table S4.

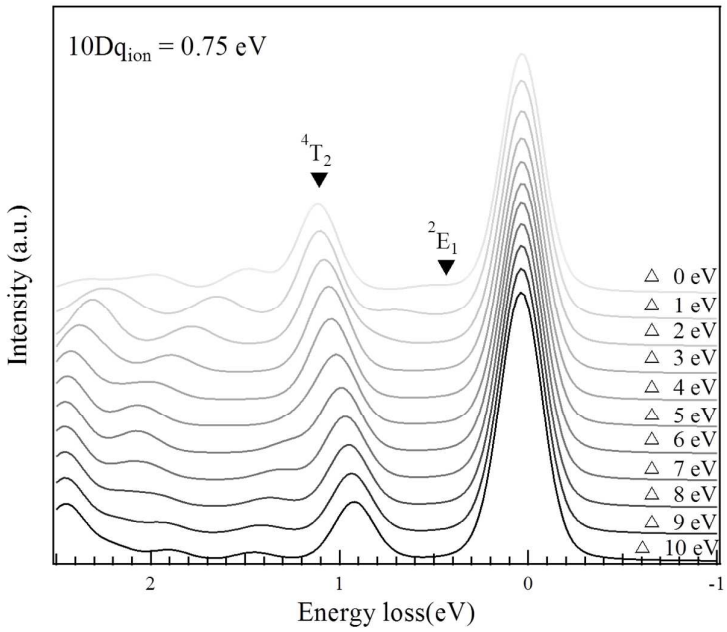

Figure S7. 2p3d RIXS spectra at a constant excitation energy with floating Δ and $10Dq_{ion}$ fixed at 0.5 eV.

Table S4. Energy Maximum of the First dd-peak in the RIXS Calculations with Different $10Dq_{ion}$ and Δ. $10Dq_{eff}$ and ΔE_{CT} were Obtained from Equation (s10) and (s11), Respectively

	$10Dq_{ion}$ = 0.5			**0.75**	**1.0**
Δ	**$^4T_1$**	**$10Dq_{eff}$**	**ΔE_{CT}**	**ΔE_{CT}**	**ΔE_{CT}**
0	0.86	0.932	0.432	0.414	0.395
1	0.85	0.921	0.421	0.414	0.395
2	0.83	0.898	0.398	0.391	0.395
3	0.80	0.863	0.363	0.367	0.372
4	0.78	0.844	0.344	0.356	0.349
5	0.75	0.805	0.305	0.321	0.325
6	0.73	0.782	0.282	0.298	0.279
7	0.72	0.770	0.270	0.263	0.256
8	0.69	0.735	0.235	0.240	0.233
9	0.67	0.712	0.212	0.229	0.210
10	0.66	0.701	0.201	0.217	0.210

c. The Effective Crystal Field Equation (Constraints)

Figure S8 shows the results according to the values in Table S3 and Table S4. Both are fit by a linear relation. The first relation is given as equation (3) in the main text:

$$\Delta E(10Dq_{eff}) = \Delta E_{^4T_1 - {}^4T_2} = 0.865 \times 10Dq_{eff} + 0.0534 \quad \text{(s10)}$$

The fitting error are about ±0.006 and ±0.005 for coefficients 0.865 and 0.0534 respectively. This is the solution without considering charge transfer effects, which can also be described in a $3d^7$ Tanabe-Sugano diagram (Figure S5). For $10Dq_{eff}$ values below 0.2 eV the difference deviates and becomes zero at $10Dq_{eff}$=0. The relation can be described by a linear equation from $10Dq_{eff}$=0.3 to 1.3eV (Figure S8 insert).

The only effect of $10Dq_{ion}$ is to split $3d^7$ and $3d^8\underline{L}$ configurations individually. So, the calculation starts from a given ionic crystal field $10Dq_{ion}$ (*i.e.* $10Dq_{eff}$ is not a simulation parameter). For example, when we consider charge transfer effects, the original ground state $|3d^n\rangle$ and the ligand hole state $|3d^{n+1}\underline{L}\rangle$ share the same total crystal field. However, $10Dq_{eff}$ includes both $10Dq_{ion}$ and ΔE_{CT}. To obtain ΔE_{CT}, we calculate the RIXS spectra as a function of Δ at three different $10Dq_{ion}$ values and use equation (s10) to optimize the new crystal field value. Approximating the relation between ΔE_{CT} and Δ as a linear function, we obtained a second relation (equation (4) in the main article):

$$\Delta E_{CT} = 10Dq_{eff} - 10Dq_{ion} \sim 0.43 - 0.0239 \times \Delta \quad \text{(s11)}$$

The fitting error are about ±0.006 and ±0.001 for coefficients 0.43 and 0.0239 respectively. From Figure S7 we find that this equation is almost independent of $10Dq_{ion}$. It implies that ΔE_{CT} is only dependent on the Δ value. Moreover, the linear model only gives a small error after applying different Δ values. As a result, we can then simulate our RIXS spectra according to these equations.

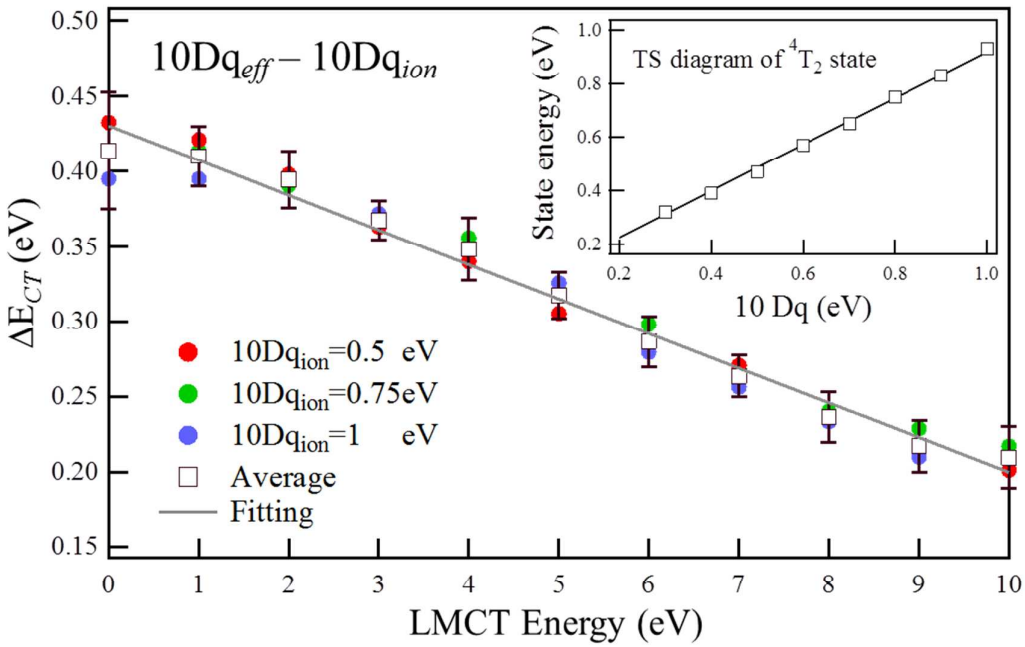

Figure S8. ΔE_{CT} correlation with respect to Δ. The colored dots correspond to series at three different fixed $10Dq_{ion}$ values and the white square reflects their average values. The black line is the fitted curve from which equation (s11) was obtained. The insert shows the energy difference between the $^4T_1$ ground state and the $^4T_2$ first dd excited as a function of 10Dq if no charge transfer is considered. The fit relation is equation (s10). The error bar is obtained by the root mean square of the difference from points to the fitting curve.

d. The Determination of Slater Integrals

Keeping the optimized 10Dq and Δ, the atomic parameters were optimized to obtain the best fit for both the 2p XAS and all 2p3d RIXS spectra, where the same parameters are used for all four systems. Figure S9 shows the simulation processes for searching the F^2_{dd} and F^4_{dd}, which were optimized as 82% and 94% of the Hartree-Fock values, respectively. On the other sides, the F^2_{pd}, G^1_{pd}, and G^3_{pd} were optimized according to 2p XAS and the values are 88%, 80%, and 88% of the Hartree-Fock respectively (Figure S10). Here we note that the optimized Slater integrals values were not exactly 80% from the atomic Hartree-Fock values.

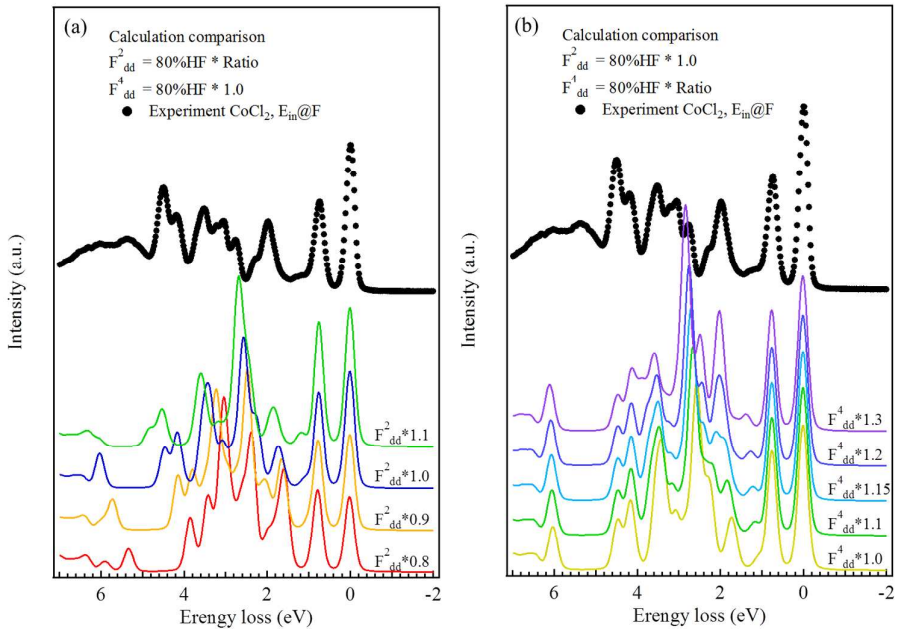

Figure S9. The optimization process of F^2_{dd} and F^4_{dd} (target on RIXS spectra of $CoCl_2$). (a) Fixed F^4_{dd} and free the F^2_{dd} values. (b) Fixed F^2_{dd} and free the F^4_{dd} values.

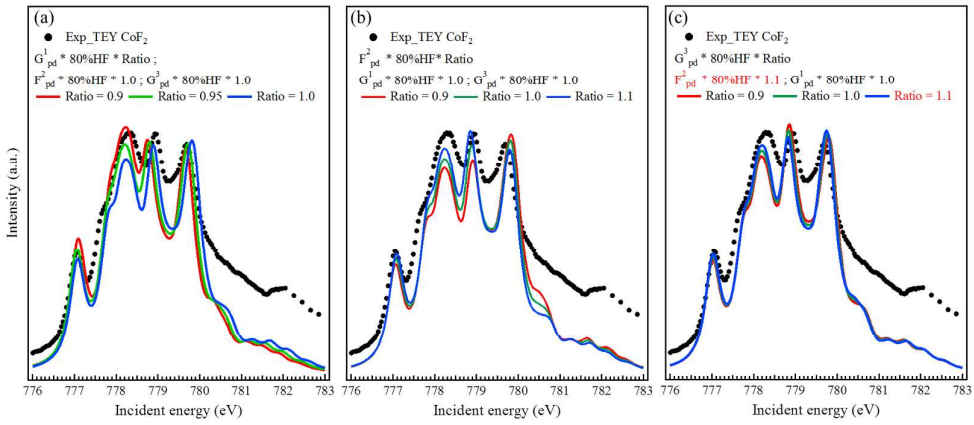

Figure S10. The optimization process of F^2_{pd}, G^1_{pd}, and G^3_{pd} values (target on XAS spectra of CoF_2). The panels focus on finding the value of (a) G^1_{pd}, (b) F^2_{pd}, and (c) G^3_{pd}.

5. Effect of the $3d^9\underline{L}^2$ Configuration

The third configuration in Co^{2+} charge transfer calculations $3d^9\underline{L}^2$, is ignored in the main article. In Figure S11 the three configurations calculation using $CoBr_2$ parameters is shown. The bonding state shows no remarkable difference between two and three configurations simulations, and the $3d^9\underline{L}^2$ configuration contribution can be ignored if only the bonding state is considered. On the other hand, the simulation with three configurations gives a smaller anti-bonding state energy, compared to the two configuration solution at fixed Δ. That is, the Δ value is about 0.3 eV larger for $CoBr_2$ as given by the calculations in the main text, bringing it closer to literature values. Note that we used 0 width for the configuration with ligand hole. In this simplified case, it reduces the calculating loading but still represent the shift of the anti-bonding states.

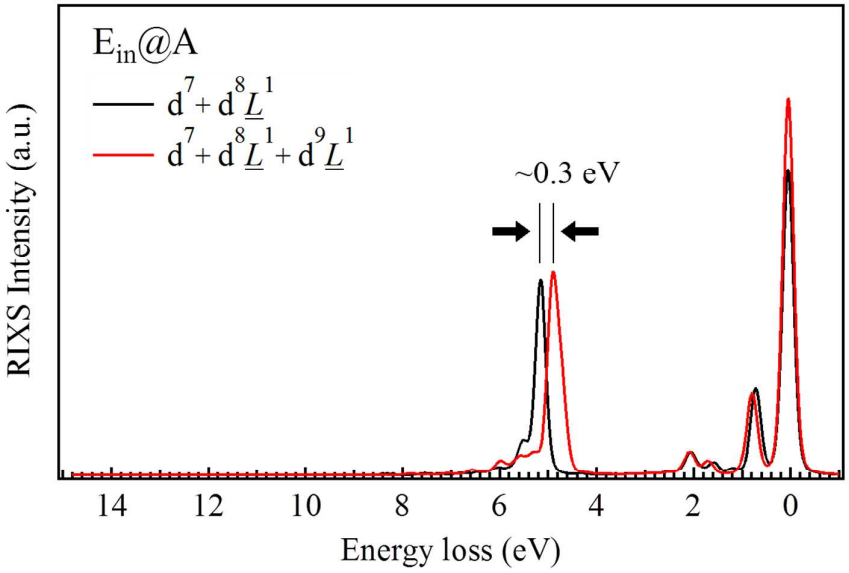

Figure S11. 2p3d RIXS simulations with two (black) and three (red) configurations using the reported $CoBr_2$ parameters.